COMPUTATIONAL STUDY OF THE EFFECT OF DIFFERENT INJECTION ANGLE ON HEAVY DUTY DIESEL ENGINE COMBUSTION

by

Ali Akbar RANJBAR, Kurosh SEDIGHI, Mousa FARHADI, and Mohsen POURFALLAH

Diesel engines exhausting gaseous emission and particulate matter have long been regarded as one of the major air pollution sources, particularly in metropolitan areas, and have been a source of serious public concern for a long time. The choosing various injection strategies is not only motivated by cost reduction but is also one of the potentially effective techniques to reduce exhaust emission from diesel engines. The purpose of this study is to investigate the effect of different injection angles on a heavy duty diesel engine and emission characteristics. The varieties of injection angle were simulated and the emissions like soot and NO is calculated. The comparison between the different injection strategies was also investigated. A combustion chamber for three injection strategies (injection direction with angles of $\alpha = 67.5$, 70, and 72.5 degree) was simulated. The comparative study involving rate of heat release, in-cylinder temperature, in-cylinder pressure, NO and soot emissions were also reported for different injection strategies. The case of $\alpha = 70$ is optimum because in this manner the emissions are lower in almost most of crank angle than two other cases and the in-cylinder pressure, which is a representation of engine power, is higher than in the case of $\alpha = 67.5$ and just a little lower than in the case of $\alpha = 72.5$.

Key words: *diesel engine, injection angle, heat release, meanmass fraction, mean soot mass fraction*

Introduction

The need for maximum fuel economy and minimum pollution and noise in diesel engines requires a detailed investigation – both experimental and numerical – on the characteristics of the fuel injection systems [1-4], but much must be done to develop very accurate mathematical models to reduce the long and expensive experimental testing.

The possibility of describing precisely the influence of the various volumes on injection permitted the simulation of new systems such as the compact injector-pump units [5]. The use of simplifying hypotheses (neglecting friction, assuming fluid velocity and density constant with pressure) permitted a theory of formulation of the propagation in pipes based on small acoustic perturbation. This is characterized by its simplicity and a sense of physics. Nevertheless, in the new systems the high pressures (more than 100 MPa) contradict the hypothesis of a constant sound velocity and call attention to phenomena like blow by losses in the gap between plunger and needle, pipe elasticity, and variation of the flow characteristics with pressure. Afterwards, interest was directed to the spray and the interrelation between its characteristics and the geometric config-

uration of the system [6-8]. The influence of different injector geometries was studied as well as the detailed simulation of the moving parts allowing the calculation of the mechanical stress. Increasing the number of nozzle holes in diesel engines has the potential to lower nitric oxides (NO_x) and CO_2. In this manner, the combustion process is modified so that more combustion occurs under lean mixture conditions which then lead to lower local combustion temperature. The absence of locally high temperatures and a rich fuel air mixture during combustion process makes simultaneous reductions of the NO_x and CO_2. As combustion takes place throughout the bulk of the lean mixture, NO_x and particulate mater (PM) emissions are much lower than those from conventional diesel combustion with diffusive combustion. The high emissions of soot are delaying the concept. The effective preparation of a homogeneous lean mixture without the formation of a partially rich mixture and the elimination of fuel deposition on the piston crown and combustion chamber wall are possible solutions that will allow the achievement of a high thermal efficiency and a reduction of the exhaust emissions. There are increases in the soot emissions which cause an increase in fuel consumption. Several modifications of the injector design including changes in the nozzle diameter, an increase in the number of nozzle holes, and a narrowing of the spray cone angle are commonly used to reduce the fuel wetting on the piston head surface and cylinder wall. Therefore, an injection with more holes strategy in direct injection (DI) diesel engine was suggested in this work. Injectors with more holes are applied to form a homogeneous fuel mixture prior to ignition. The aim of this study was to investigate the effect of injectors with more holes on the exhaust emissions of a DI diesel engine.

Model formulation

Especially in diesel engines there is a strong interaction of mixture formation and combustion since both processes occur simultaneously. The most important phenomena are the liquid core atomization, the collision and secondary break-up of fuel droplets, their momentum, energy and mass exchange with the gas phase, and the droplet-wall-interaction. Simultaneously, numerous complex chemical reactions occur, which initiate the auto ignition, the burnout of the premixed phase and the subsequent turbulent non-premixed combustion. It is a demanding task for the numerical simulation tools to adequately describe all the above phenomena, which are physically divers, but strongly interactive. The numerical simulation of flow and mixture formation is based on an Eulerian description of the gas-phase and on a Lagrangian description of the droplet-phase. The interaction between both phases is described by source terms for the momentum, heat and mass exchange. This methodology has widely been used for spray modeling and is also implemented in the computational fluid dynamics (CFD) code FIRE [9]. The turbulent gas flow is described by a numerical solution of the complete ensemble averaged equations of the conservation of mass, momentum, energy, and species mass fraction in an unstructured numerical mesh. Turbulence is modeled using a standard k-ε model.

Spray submodels

Spray simulations involve multi-phase flow phenomena and as such require the numerical solution of conservation equations for the gas and the liquid phase simultaneously. With respect to the liquid phase, practically all spray calculations in the engineering environment today are based on a statistical method referred to as the discrete droplet method (DDM) [10]. This operates by solving ordinary differential equations for the trajectory, momentum, heat and mass transfer of single droplets, each being a member of a group of identical non-interacting droplets termed a parcel. Thus one member of the group represents the behavior of the complete parcel.

Droplet parcels are introduced in the flow domain with initial conditions of position, size, velocity, temperature, and number of particles in the parcel. Introduction of droplets is emerging from a nozzle as a spray and entering the flow domain through the inlet areas as a gas/liquid mixture. The atomization process of sprays is accounted for with distinctive submodels. The droplet-gas momentum exchange, turbulent dispersion, evaporation of droplets, secondary break-up, droplet collision, and droplet-wall interaction are covered with a comprehensive set of models. The vapor of evaporating droplets is used as a source term of an additional transport equation for the vapor void fraction in Eulerian formulation.

The droplets are tracked in a Lagrangian way through the computational grid used for solving the gas phase partial differential equations. Full two-way coupling (interaction) between the gas and liquid phases is taken into account. In situations of negligible influence of the dispersed phase on the continuous one, the gas phase flow can be simulated in advance and the droplet simulation can be performed afterwards.

Basic equations

The differential equations for the trajectory and velocity of a particle parcel are as follows.

Momentum

$$m_d \frac{du_{id}}{dt} = F_{idr} \tag{1}$$

where F_{idr} is the drag force, given by:

$$F_{idr} = D_p u_{irel} \tag{2}$$

where D_p is the drag function, defined as:

$$D_p = \frac{1}{2} \rho_g A_d C_D |u_{rel}| \tag{3}$$

where C_D is the drag coefficient which generally is a function of the droplet Reynolds number Re_d and A_d is the cross-sectional area of the particle.

From the various formulations in literature for the drag coefficient of a single sphere, we used the following formulation from [11]:

$$C_D = \frac{24}{Re_d}(1 + 0.15\,Re_d^{0.687}) \qquad Re_d < 10^3 \tag{4}$$

and

$$C_D = 0.44 \qquad Re_d > 10^3 \tag{5}$$

The particle Reynolds number is shown in the following equation where μ_g is the domain fluid viscosity:

$$Re_d = \frac{\rho_g |u_{rel}| D_d}{\mu_g} \tag{6}$$

Inserting above force and relations into eq. (1) and dividing it by the particle mass the equation for the particle acceleration as used by default is:

$$\frac{du_{id}}{dt} = \frac{3}{4} C_D \frac{\rho_g}{\rho_d} \frac{1}{D} |u_{ig} - u_{id}| (u_{ig} - u_{id}) \tag{7}$$

which can be integrated to get the particle velocity and from this the instantaneous particle position vector can be determined by integrating:

$$\frac{\mathrm{d}x_{\mathrm{id}}}{\mathrm{d}t} \quad u_{\mathrm{id}} \tag{8}$$

Break-up model

Hear the break-up model is wave standard. The growth of an initial perturbation on a liquid surface is linked to its wavelength and to other physical and dynamic parameters of the injected fuel and the domain fluid [12].

There are two break-up regimes, one for high velocities and one for low velocity Rayleigh type break-up. For the first case the size of the product droplets is set equal to the wavelength of the fastest growing or most probable unstable surface wave. Rayleigh type break-up produces droplets that are larger than the original parent drops. This regime is not important for high pressure injection systems.

Turbulence dispersion

As particles pass through the flow it is assumed that they interact with the individual turbulent eddies. Each interaction deflects the particle as dictated by the instantaneous velocity of the turbulent eddy and the particle inertia. These additional turbulence effects on the spray particles cannot be resolved by the flow field in detail so a turbulent dispersion model is used. The particle trajectory is determined similar to a random walk computation until the particle passes out of the region under consideration. The instantaneous gas velocity within a turbulent eddy is obtained from the mean domain fluid velocity u_{ig} and the turbulence kinetic energy k. Both are known from the solution of the gas phase equations. The interaction time of a particle with the individual eddies is estimated from two criteria, the turbulent eddy life time and the time required for a particle to cross the eddy.

In the stochastic dispersion method employed by Gosman *et al*, [13], the effects of turbulence on the spray particles are modeled by adding a fluctuating velocity u_i to the mean gas velocity u_{ig}. Assuming isotropic turbulence the components of the particle fluctuating velocity is determined randomly from a Gaussian distribution with standard deviation $\sigma = (2k/3)^{1/2}$ where k is the turbulence kinetic energy of the gas at the particle location:

$$u_i \quad \frac{2}{3}k^{1/2} \mathrm{sign}(2Rn_i \quad 1)\,\mathrm{erf}^{-1}(2Rn_i \quad 1) \tag{9}$$

where Rn_i is a random number in the range from $[0 < Rn_i < 1]$ for each vector component and erf^{-1} is the inverse Gauss function.

The fluctuation velocity u_i is chosen as a piecewise constant function of time and is updated when the turbulence correlation time t_{turb} has passed. The turbulence correlation time t_{turb} is the minimum of the eddy break-up time and the time for the particle to traverse an eddy, and is given by:

$$t_{\mathrm{turb}} \quad \min \quad C_\tau \frac{k}{\varepsilon}, \quad C_1 \frac{\sqrt{k^3}}{\varepsilon} \frac{1}{|u_{\mathrm{g}} \quad u \quad u_{\mathrm{d}}|} \tag{10}$$

where $C_\tau = 1.0$ and $C_1 = 0.16432$ are model constants.

The case that the computational time step δt is larger than the turbulence correlation time t_{turb} the spray integration time step is reduced to t_{turb}.

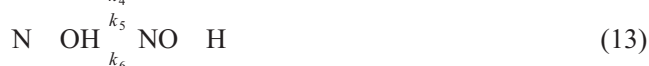**Emission submodels**

NO formation

At present, a global chemistry model [14] together with an *a priori* assumed temperature PDF (probability density function) is available for the evaluation of the mean reaction rate of nitric oxide formation. Complex kinetic mechanisms are applicable only for simple flame computations (*e. g.* one-dimensional, laminar, *etc*.). For real turbulent flame calculations, their use is impractical due to the complexity of the interacting processes (turbulence, radiation, heat transfer, *etc*.) which must be considered to obtain realistic results. Therefore, simplified approaches must be used for complex applications, whereby essential information is not lost due to the reduction procedure [15, 16]. A model derived by systematic reduction of multi-step chemistry is used for the evaluation of the nitric oxide formation. This reduction is based on the partial equilibrium assumption of the considered elementary reactions using the extended Zeldovich mechanism describing the thermal nitrous oxide formation.

Zeldovich model

In general, the nitric oxide (NO) formation stems from three principal sources:
– thermal NO which is formed due to the dissociation of the molecular air-nitrogen [17-19],
– prompt NO (Fenimore NO) formed by the "attack" of hydrocarbon fragments on the air-nitrogen [17], and
– NO formed from nitrogen containing components in the fuel.

Fuel-NO formation can be neglected during the combustion process in internal combustion engines. Prompt NO formation can also be neglected since this process plays no dominant role in comparison to the thermal NO formation (less than 5% of is produced via this path) [19, 20]. NO is formed in both the flame front and post-flame gases. In engines, the cylinder pressure rises during the combustion process, so earlier burnt gases are compressed to a higher temperature level as they have immediately after their combustion. Hence, the thermal NO formation in the burnt gases always dominates in comparison to the NO formed in the flame front and represents the main source of the nitric oxide in engines whose reaction paths are effective at high temperatures (more than 1600 K). The reaction mechanism can be expressed in terms of the extended Zeldovich mechanism:

$$N_2 + O \underset{k_2}{\overset{k_1}{\rightleftharpoons}} NO + N \tag{11}$$

$$N + O_2 \underset{k_4}{\overset{k_3}{\rightleftharpoons}} NO + O \tag{12}$$

$$N + OH \underset{k_6}{\overset{k_5}{\rightleftharpoons}} NO + H \tag{13}$$

The first reaction represents the rate limiting step in comparison to the other reactions. A very high activation energy (or temperature) is necessary to decompose the stable triple-bond of the molecular air-nitrogen. Accordingly, this reaction is significantly fast at high temperatures. In principal, it can be seen that the thermal NO formation is mainly determined by only five chemical species (O, H, OH, N, and O_2) but not by the fuel being used. In order to obtain the required concentrations of the radicals, a complex reaction mechanism must be used in order to determine NO concentration. In the literature different possibilities are suggested to represent the rate law for NO [21, 22].

An irreversible single-step reaction mechanism is used for the conversion of fuel, involving only stable molecules such as C_nH_m (as fuel), O_2, CO_2, H_2O, and N_2. Hence, an approach is implemented based on these stable molecules in order to predict thermal NO. The maximum of NO appears at an equivalence ratio of about 0.9, *i. e.* slightly fuel-lean. In most stoichiometric and fuel-lean flames, the occurring OH concentration is very small. Using this fact, the third reaction of the Zeldovich mechanism can be neglected. In addition, the characteristic times [22] for the formation of thermal NO is several orders of magnitude slower than those characteristic times of the combustion process. Hence, the combustion and the NO formation processes can be assumed to be decoupled and therefore, the concentrations of O_2, N, O, OH, and H can be approximated by an equilibrium assumption. If the assumption is made that the thermal NO formation starts at considerably high temperatures (due to the decomposition of the stable triple-bond of N_2) a partial equilibrium of the first two reactions can be assumed. An analysis of experiments and simulations indicates that at high temperatures ($T > 1600$ K) the reaction rates of the forward and reverse reactions are equal.

The state of the considered reaction is said to be in partial equilibrium where the reaction couples are in equilibrium. Using these assumptions, the concentrations of radicals can be expressed in terms of the concentrations of stable molecules (since they are easier to measure). These are present in much larger concentrations than the radicals. The assumption of partial equilibrium provides satisfactory results only at considerably high temperatures, since at temperatures less than 1600 K a partial equilibrium is not established.

For the formation of thermal NO, the partial equilibrium approach can be used and so the equilibrium of the first two reactions can be expressed as follows by:

$$k_1[N_2][O] = k_2[NO][N] \tag{14}$$

$$k_2[N][O_2] = k_4[NO][O] \tag{15}$$

Using these expressions, the equation system can be solved and results in a global reaction approach for the thermal NO formation which can be expressed as:

$$N_2 + O_2 = 2NO \tag{16}$$

with $k_f = k_1 k_3$ as the forward and $k_b = k_2 k_4$ as reverse reaction rate. The chemical species appearing in this global reaction is also used in the given single-step fuel conversion equation. Hence, the source term in the conservation equation for NO is obtained via:

$$\frac{d[NO]}{dt} = 2k_f[N_2][O_2] \tag{17}$$

where only the formation (therefore, only the forward reaction) is considered. The reaction rate of the forward reaction is given as:

$$k_f = \frac{A}{\sqrt{T}} \exp\left(\frac{E_a}{RT}\right) \tag{18}$$

where A is the pre-exponential factor and E is the activation energy.

Soot emissions

Under high temperature and fuel rich conditions, as typically found in diesel combustion, hydrocarbon fuels exhibit a strong tendency to form carbonaceous particles – soot. Usually, under engine running conditions, most of the soot formed in the early stages of the combus-

tion process is depleted due to oxidation. This takes place in oxygen rich areas of the combustion chamber later in the engine cycle. In diesel engines, it is the amount and completeness of the soot oxidation process that actually determines the engine particle emission characteristics. The formation of particulates involves a large number of different chemical and physical processes, like the formation and growth of large aromatic hydrocarbons, their subsequent conversion to particles, the coagulation of primary particles, and the growth of solid soot particles due to the accumulation of gaseous components [23, 24]. Soot particle formation process is characterized by a gaseous-solid conversion, whereby the solid phase does not exhibit a uniform chemical and physical topology.

It is evident that the formation of soot, *i. e.* the conservation of hydrocarbon rich, aliphatic compounds involving only a relatively small number of carbon atoms into an agglomerate comprising millions of them, is the result of a highly complex chemical process involving hundreds of reactions and as many intermediate and radical species. Particle oxidation mainly occurs due to the attack of atomic oxygen onto the carbonaceous particles under high temperature conditions. In spite of the great complexity of the underlying processes, the individual reactions contributing to the soot formation and oxidation rates can be related to known flame parameters, such as fuel mass fraction, partial pressure of oxygen, flame temperature and/or turbulent mixing intensity. Under ideal conditions, the combustion of hydrocarbon fuels forms CO_2 and H_2O. The necessary amount of oxygen is the stoichiometric oxygen requirement $O_{2\,st}$ calculated from the following equation:

$$C_n H_m + \left(n + \frac{m}{4}\right) O_2 \rightarrow nCO_2 + \frac{m}{2} H_2O \tag{19}$$
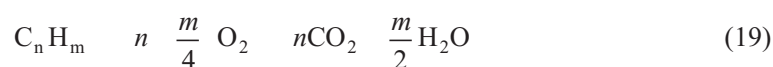
So for ideal combusting of 1 mole $C_n H_m$, $(n + m/4)$ moles O_2 is required. This ideal amount of oxygen is called $O_{2\,st}$.

The real amount of oxygen, available for the combustion, is expressed by the air access ratio $\lambda = O_2/O_{2\,st}$ or by the equivalence ratio:

$$\varphi = \frac{1}{\lambda} = \frac{O_{2\,st}}{O_2} \tag{20}$$

For conditions at equivalence ratios $\varphi > 1$, there is a big potential for soot formation.

There are four major processes in soot formation: nucleation, coagulation, surface growth, and oxidation [23, 24]. Stagnation of premixed flames shows that the fuel molecules are split into radicals, mainly acetylene. Subsequently this 2-D radical grows by chemical reactions, H abstraction, and acetylene addition. This process forms large aromatic rings out of aliphatic species. In further steps the molecules become 3-D and form carbonaceous particles by coagulation. Through gaseous-solid conversion, the soot particles grow afterwards (surface growth). A similar process is running in diffusion flames, but highly influenced by the inhomogeneous mixture and turbulent mixing. The most important parameters during the soot formation are the local air/fuel ratio (C/H ratio and C/O ratio), temperature, pressure, and residence time.

The combustion chamber specifications

A heavy duty diesel engine combustion chamber with the bowl shape of fig. 1 is modeled.

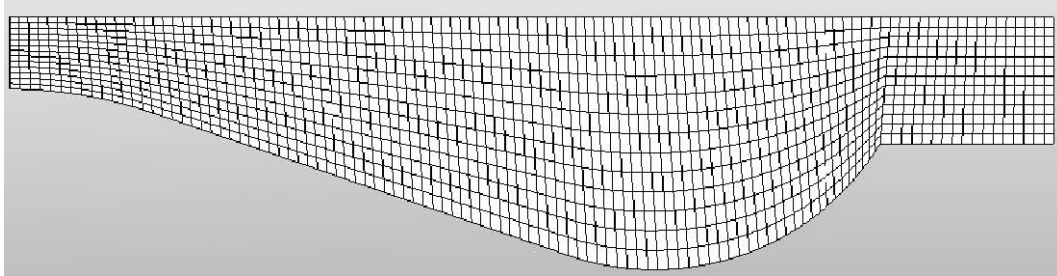The engine related specification has been presented in tab. 1.

Figure 1. Section of combustion chamber

The specifications of the spray have been summarized in tab. 2.
Figure 2 shows the 60°-sector computational mesh in 3-D.

Table 1. Engine specifications

Type	Single cylinder, turbocharged direct injection
Bore [mm]	165
Stroke [mm]	195
Compression ratio	13
Engine speed [rpm]	1800

Table 2. Spray characteristics

Type	Common rail, direct injection with single central injector
Number of nozzle orifice	6
Nozzle orifice diameter [mm]	0.32
Start of injection (aTDC) [deg]	−17
Injection period (CA) [deg]	31.8
Injection mass [mg per cycle]	77

Since a 6-hole nozzle is used, only a 60° sector has been modeled. The current grid contains 15130 cells and an additional grid with 24089 has been created in order to perform a sensitivity analysis of the grid resolution on combustion and emissions formation.
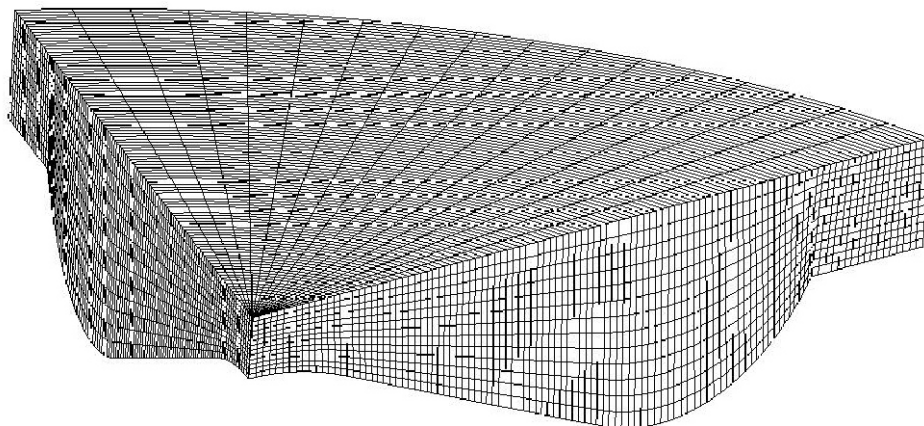
Figure 2. 60°-sector computational mesh

Average cylinder pressure, temperature, NO_x, and soot formation rate predictions were compared between the 2 grid resolutions. In fig. 3 the cylinder pressure comparison is shown and the predictions are almost identical for all tow cases. Similar results are obtained for the average cylinder temperature. The NO_x and soot emissions, at the end exhaust valve opening (EVO) were also compared. Therefore, the coarse grid containing 15130 cells will be used in this work for analysis of mixture and emissions formation.
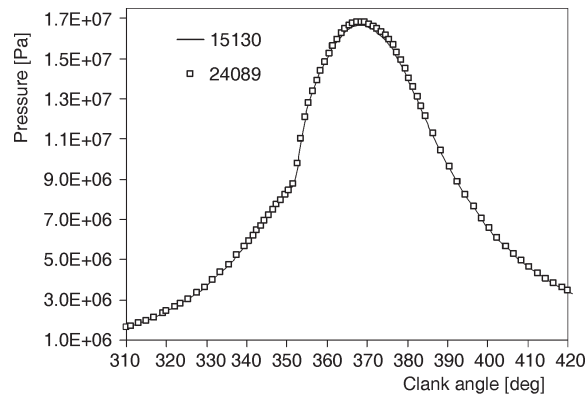
Figure 3. Grid sensitivity analysis: cylinder pressure comparison

Model validity

Because the target engine is new generation engine and it is under development, we used another heavy duty diesel engine that named Caterpillar 3406 which is tested in [25].The specification of experimental diesel engine is listed in tab. 3. Figures 4 and 5 shows the differences between experimental and numerical results of in-cylinder pressure and heat release.

These results show good agreement between experimental and modeling case and it is not a wrong that this model can be predict the engine performance and emission near real conditions.

Table 3. Caterpillar 3406 specification

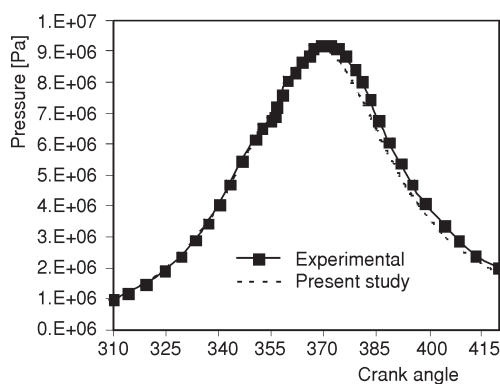| Bore [mm]	137.19
Stroke [mm]	165.1
Compression ratio	15
Piston crown	Mexican hat
Engine speed [rpm]	1600
Fuel rate [g per minute]	135
Number of nozzle orifice	6
Nozzle orifice diameter [mm]	0.259
Spray angle	62.5

Figure 4. Comparison between experimental and modeling in-cylinder pressure
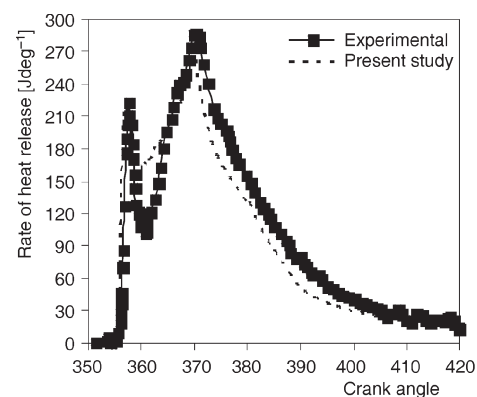

Figure 5. Comparison between experimental and modeling heat release

Results and discussions

There are three injection strategies; injection with angles of 72.5, 70, and 67.5 degree, respectively. See fig. 6.
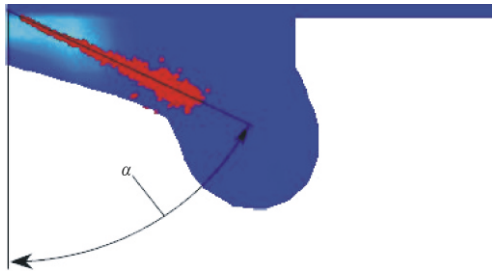

Figure 6. A combustion chamber cross-section by the plane determined by cylinder and spray axes (color image see on our web site)
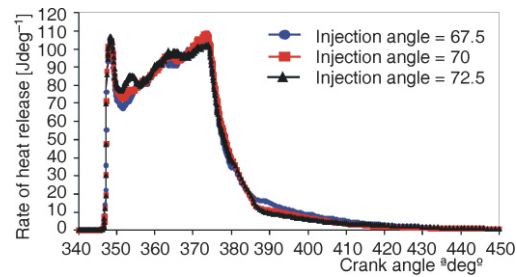

Figure 7. Heat release rates as a function of crank angle generated by varying fuel injection angle (color image see on our web site)

Figure 7 indicates the rate of heat release against various degrees of crank angle. A few degree of crank angle after beginning of the injection, an increase in heat releases is appeared suddenly. This is because of premixture of high amount of fuel with air. After this sudden increase to about 105 J/deg, the rate of heat release is confined between 70 to 110 J/deg.
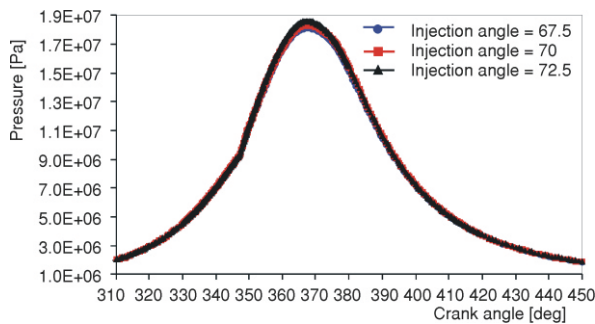
As shown in figs. 8 and 9 large injection angle leads to the increase of air entrainment into the fuel spray because of the longer spray path before impinging piston bowl. Therefore, the cylinder pressure and temperature are highest in the case of injection angle 72.5 deg.

Figure 8. Mean in-cylinder pressure as a function of crank angle generated by varying fuel injection angles (color image see on our web site)
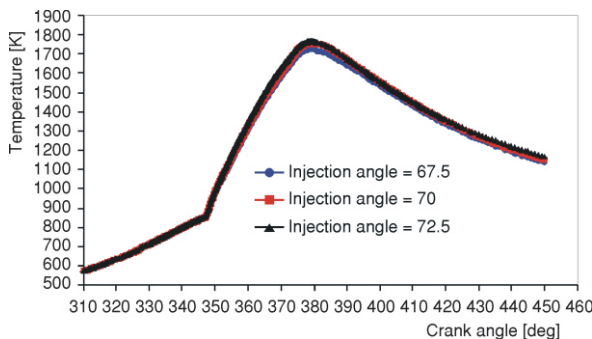

Figure 9. Mean in-cylinder temperature as a function of crank angle generated by varying fuel injection angles (color image see on our web site)

Figure 10 shows the produced NO in combustion chamber. The results indicate that by increasing the injection angle, the NO increases. This phenomena is justified by observing fig. 9. In that figure by increasing the injecting angle the temperature of the combustion chamber increase, so the rate of producing NO increases. By increasing injection angle the post flame region increases. As NO is produced in post flame region so, the probability production increases in the case of injection angle with higher degree.

By decreasing injection angle soot formation increases because the cone

flame is near wall and exposure to lower temperature. Although because of high oxidation the soot disappear near 400 deg for all three cases, fig. 11.

Conclusions

In the present study the diesel combustion has been simulated and the effect of the injection angle on DI diesel engine combustion and emission formation was investigated. Results were validated and compared with available experimental data for Caterpillar DI diesel engine for mean cylinder pressure, rate of heat release, and exhaust emission. A good agreement between the predicted and experimental values ensures the accuracy of the numerical predictions collected with the present work.

Optimum fuel consumption and pollutant decrease in internal combustion engine are two substantial parameters. Optimization procedures are used for decreasing the production expenses instead of post-treatment methods. Injection angle is one of the parameters which effect on combustion and producing pollution. In this study three geometries are chosen base on previous experimental results.

Figure 10. Mean NO mass fraction as a function of crank angle generated by varying fuel injection angles (color image see on our web site)

Figure 11. Mean soot mass fraction as a function of crank angle generated by varying fuel injection angles (color image see on our web site)

According to the indicated result in table 4, pressure and temperature raised to 186 bar and 1761 K, respectively, in 72.5 degree of injection angle. Lower soot and higher show the better combustion in this injection angle. This means that injection angle must be well matched to the combustion chamber.
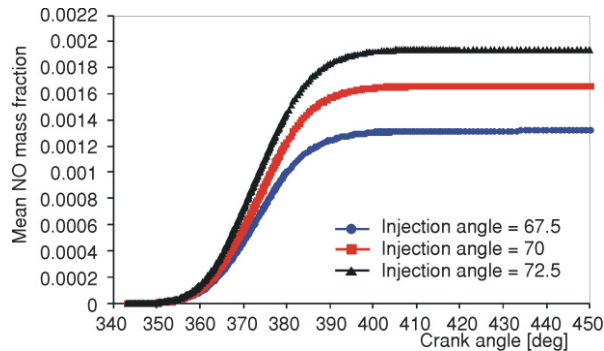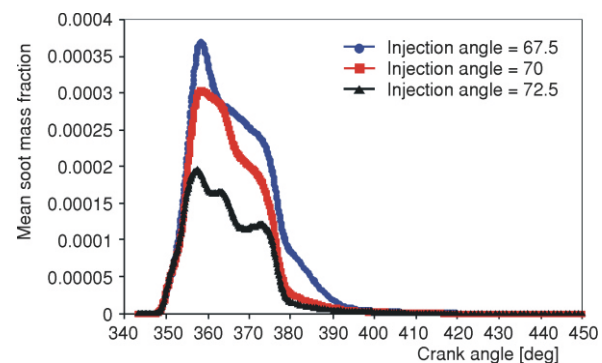
Table 4. CFD summary results of injection angle study

Calculated characteristic parameters	Injection angle		
	67.5 deg	70 deg	72.5 deg
Max cylinder presure [bar]	181	183	186
Point of max. cylinder pressure	8 (aTDC)	8 (aTDC)	8 (aTDC)
Max. cylinder temperature [K]	1723	1757	1761
Point of max. cylinder temperature	20 (aTDC)	20 (aTDC)	20 (aTDC)
NO at EVO (mass fraction)	0.001318	0.0012662	0.001940
Soot at EVO (mass fraction)	1.89E-0.8	4.07E-10	1.27E-11

Acknowledgment

Nomenclature

a – stoichiometric relations, [–]
C_D – drag coefficient, [–]
c_{pd} – specific heat of liquid, [$Jkg^{-1}K^{-1}$]
c_τ – constant due to Lagrangian time scale, [–]
D_p – drag function
F_i – source vector, [N]
k – turbulence kinetic energy, [m^2s^{-2}]
k – reaction rate, [ls^{-1}]
m_d – particle mass, [kg]
Re_d – particle Reynolds number, [–]
t_{turb} – turbulence interaction time, [s]
u_{id} – particle velocity vector, [ms^{-1}]
u_{ig} – domain fluid velocity, [ms^{-1}]

x_{id} – particle position vector, [m]

Greek letters

ε – dissipation rate, [m^2s^{-2}]
ρ – density, [kgm^{-3}]

Subscripts

d – droplet
dr – drag
g – gas (ambient) conditions
p – particle
rel – relative
st – stoichiometric

References

[1] Kato, T., *et al.*, Spray Characteristics and Combustion Improvement of D. I. Diesel Engine with High Fuel Injection, SAE paper No. 890265, 1989
[2] Oblaender, K., *et al.*, The Influence of High Pressure Fuel Injection Diesel Engine, SAE paper No. 890438, 1989
[3] Itoh, S., Sasaki, S., Arai, K., Advanced in-Line Pump for Medium-Duty Diesel Engine to Meet Future Emissions Regulations, SAE paper No. 910185, 1991
[4] Okajima, M., *et al.*, Contribution of Optimum Nozzle Design to Injection Rate Control, SAE paper No. 910185, 1991
[5] SchuUen, R., Hames, R., Computer Simulation of the GM Unit Injector, SAE paper No. 780161, 1978
[6] Marcic, M., Kovacic, Z., Computer Simulation of the Diesel Fuel Injection System, SAE paper No. 851583, 1985
[7] Gibson, D. H., A Flexible Fuel Injection Simulation, SAE paper No. 861567, 1986
[8] Kumar, K., *et al.*, A Finite Difference Scheme for the Simulation of a Fuel Injection System, SAE paper No. 831337, 1983
[9] ***, FIRE Combustion, Spray and CFD Solver User Manual, v. 8.3, 2004
[10] Dukowicz, J. K., A Particle-Fluid Numerical Model for Liquid Sprays, *J. Comp. Physics, 35* (1980), 2, pp. 229-253
[11] Schiller, L., Naumann, A. Z., Drag Coefficient Correlation, VDI Zeitschrift, *77* (1933), pp. 318-320
[12] Liu, A. B., Reitz, R. D., Modeling the Effects of Drop Drag and Break-up on Fuel Sprays, SAE paper No. 93007
[13] Gosman, A. D., Ioannides, E., Aspects of Computer Simulation of Liquid-Fueled Combustors, AIAA paper 810323, 1981
[14] Jones, W. P., Lindstedt, R. P., Global Reaction Schemes for Hydrocarbon Combustion, *Combustion and Flame, 73* (1988), 3, pp. 233-249
[15] Lam, S. H., Reduced Chemistry Modeling and Sensitivity Analysis, Lecture Notes for Aerothermochemistry for Hypersonic Technology, Lecture Series Program at the Von Karman Institute for Fluid Dynamics, Brussels, Belgium, 1995
[16] Maas, U., Pope, S. B., Simplifying Chemical Kinetics; Intrinsic Low-Dimensional Manifolds in Composition Space, *Combustion and Flame, 88* (1992), 3-4, pp. 239-264

[17] Bowman, C. T., Chemistry of Gaseous Pollutant Formation and Destruction, in: Fossil Fuel Combustion, A Source Book (Eds. W. Bartok, A. F. Sarofim), John Wiley and Sons, New York, USA, 1991, pp. 215-260

[18] Hanson, R. U., Salimian, S., Survey of Rate Constants in the N/H/O-System, in: Combustion Chemistry, (Ed. W. C. Gardiner Jr.), Springer Verlag, New York, USA, 1984, pp. 361-421

[19] Polifke, W., Fundamental and Practical Limitations of NO_x, Reduction in Lean-Premixed Combustion, Notes for the Euro Conference RWTH about Premixed Turbulent Combustion: Introduction of the State of the"ART", Aachen, Germany, 1995, pp. 1-17

[20] Zeldovich, Y. B., Sadovnikov, P. Y., Frank-Kamenetskii, D. A., Oxidation of Nitrogen in Combustion (in Russian), (Translation by M. Shele), Academy of Sciences of USSR, Institute of Chemical Physics, Moscow-Leningrad, 1947

[21] Bogensperger, M., A Comparative Study of Different Calculation Approaches for the Numerical Simulation of Thermal NO Formation, Diss. U. Graz, Austria, 1996

[22] Heywood, J. B., Internal Combustion Engine Fundamentals, McGrawHill Book Company, Second Series, 1988

[23] ***, Soot Formation in Combustion: Mechanisms and Models (Ed. H. Bockhorn), Springer-Verlag, Berlin, 1994

[24] Bockhorn, H., *et al*., Investigation of the Surface Growth of Soot in Flat Low Pressure Hydrocarbon Oxygen Flames, *Proceedings*, 20th International Symposium on Combustion, The Combustion Institute, Pittsburgh, Penn., USA, 1985

[25] Tow, T., Pierpont, A., Reitz, R. D., Reducing Particulates and NO_x Emissions by Using Multiple Injections in a Heavy Duty D. I. Diesel Engine, SAE paper 940897, 1994

Authors' affiliations:

A. A. Ranjbar,
Faculty of Mechanical Engineering,
Babol Noshirvani University of Technology
Babol, Iran

K. Sedighi
Faculty of Mechanical Engineering,
Babol Noshirvani University of Technology
Babol, Iran

M. Farhadi (**corresponding author**)
Faculty of Mechanical Engineering,
Babol Noshirvani University of Technology
Babol, Iran
E- mail: mfarhadi@nit.ac.ir

M. Pourfallah
Faculty of Mechanical Engineering,
Babol Noshirvani University of Technology
Babol, Iran